Adsorption of Gold onto γ–aminopropyltriethoxysilane Grafted Coconut Pith

[1]Muhammad Usman, [1, 2] Javaid Akhtar* and [3]Javed Iqbal
[1]School of Chemical Engineering, The University of Faisalabad, West Canal Road, Faisalabad
[2]Centre for Coal Technology, University of the Punjab, Lahore
[3]Department of Chemical Engineering, COMSATS Institute of Information Technology, Lahore, Pakistan
sweetsanwal@yahoo.com*

(Received on 7th June 2016, accepted in revised form 5th July 2017)

Summary: This study was carried out to investigate adsorption kinetic and adsorption thermodynamics of Au(III) ions onto γ–aminopropyltriethoxysilane grafted coconut pith. The results from equilibrium adsorption were fitted in various adsorption isotherm models such as Langmuir, Freundlich, Temkin and Dubinin-Radushkevich and the best fit for the experimental data was Langmuir isotherm. The maximum adsorption capacity for virgin coconut pith (VCP) and the grafted coconut pith (GCP) were 256.41 and 285.59 mg/g, respectively. The kinetic data was verified using pseudo-first-order, pseudo-second-order, elovich equation and intraparticle diffusion model. The correlation results suggested that the pseudo-second-order model fits the experimental data well. A thermodynamic study revealed the endothermic nature of reaction due to positive enthalpy (ΔH^o) values and negative values of Gibbs free energy (ΔG^o) describes the spontaneity of adsorption process. The regenerability of VCP and GCP adsorbents were investigated with NaOH (1.0 M).

Keywords: Coconut pith; Isotherm models; Thermodynamics; Kinetic models; Gold.

Introduction

Gold belonging to precious metal group has certain characteristics such as: high electrical conductivity, chemical stability and excellent resistance to corrosion, which makes it very attractive for its application in various industries; moreover, it has been extensively used in jewelry and also in medical equipments [1]. Therefore, in recent years, there has been an increase in gold concentrations from various sources such as: wastewater streams of various industries like mining [2, 3], ore and metal processing [4], electrical and electronic manufacturing [5, 6] and e-waste recycling [7, 8]. The major contribution in the electrical and electronic waste (e-waste) is from printed circuit board (PCB) containing several precious metals (i.e., gold, silver and palladium) as exhibited in Table-1 [9]. Billions of people round the globe are using cellular phones as fast communication device. The life span of these devices is decreasing due to the most users upgrade to new technology, design and style. In 2005, it was estimated that 500 million mobile phones weighing 250,000t were ready for disposal [10].

Table-1: Analysis of metals in PCB [9].

Component	Wt.%	value[a] (£/kg)	Intrinsic value of PCB	
			(£/kg of PCB)	%
Gold	0.025	142000.00	3.55	65.4
Palladium	0.010	6200.00	0.62	11.4
Silver	0.100	250.00	0.25	4.6
Copper	16.0	3.30	0.53	9.7
Aluminum	5.0	1.20	0.06	1.1
Iron	5.0	0.10	0.01	0.1
Tin	3.0	8.10	0.24	4.5
Lead	2.0	1.30	0.03	0.5
Nickel	1.0	13.20	0.13	2.4
Zinc	1.0	1.20	0.01	0.2

[a] Metal values are based on December 2007 London Metal Exchange (LME) levels.

Thus, there is an urgent need of recycling waste mobile phones to protect the environment and resource conservation [11]. It is indicated that e-waste contains large amounts of precious metals from their respective ores and can be considered as a secondary source of these valuable metals [12,13]. However, it requires an efficient system to recover, reuse and recycle gold due to its limited and continuously depleting sources [14]. There are various technologies engaged for the gold recovery such as: hydrometallurgical (ion exchange resin [15], solvent extraction [16] and precipitation [17]) and pyro-metallurgical [7] (incineration and smelting in a furnace), however, the application of these processes has some drawback, which are high cost, labor and time extensive. Therefore, these processes were not seen as efficient processes for metal recovery and the search continues for a process that can replace these techniques and should be effective, economical and environmentally benign. Biosorption process in seen as an alternative process in which biomass based adsorbents is applied for the separation and recovery of precious metals. This process draws attention due to its attractive features such as: high efficiency, low cost and simple operation [18-20]. An industrial crop produces huge quantities of cheap material during their reaping and processing of food crops [21]. A tragic situation rises as most of the lignocelluloses are eliminated by burning, which is even banned in developing areas and considered a threat to environment [22]. Different types of adsorbents have been used for Au(III) adsorption, including chemically modified chitosan [23], lignophenol gel [24], rice husk carbon [25], alfalfa [26], egg shell

---

[*]To whom all correspondence should be addressed.

membrane [27], sulfur derivatives of chitosan [28], calcium alginate beads [29], dealginated seaweed waste [30] and immobilized fungal biomass [31]. However, the emphasize in to utilize low-cost and naturally abundant materials for the recovery of gold from its source i.e., electronic and electroplating factories wastewater [1].

In this study, an organosilane, γ-aminopropyltriethoxysilane (γ-APS) with the chemical formula ($NH_2(CH_2)_3Si(OC_2H_5)_3$) was applied as coupling agent with the general formula R-Si-X_3, where R denotes the organic moiety and X denotes an oxyalkyl group [32]. The modification effect of γ-aminopropyltriethoxysilane (γ-APS) on coconut pith was investigated for the uptake of gold. The kinetic and isotherm models were applied on experimental data to elaborate the adsorption mechanism. The regenerability study was conducted by suitable eluting agent (NaOH) to enhance reusability and attractiveness of the adsorption process.

Experimental

Materials and Reagents

The biomass (coconut pith) used in the experiment was purchased from the T&H sdn. Bhd, Johor Malaysia. The sodium hydroxide (NaOH pellets) used in desorption studies was acquired from Merck and nitric acid (HNO_3) was bought from sigma-Aldrich. Ethanol and toluene were purchased from sigma Aldrich. Silane coupling agent (γ-APS) was purchased from Power Chemical Corporation (China). Gold (III) chloride ($AuCl_3$) of purity 99% was purchased from sigma-Aldrich. All the chemicals were analytical grade, except γ-APS, which was industrial grade.

Preparation of Adsorbent

Raw coconut pith was first grounded, sieved to obtain the desired particle size (0.075-0.150 mm) and later on washed to remove coloration and dirt particles. In this study, dewaxing was used as a pretreatment process to remove low molecular weight substance such as: waxes, therpenes and other impurities from coconut pith. The coconut pith was soxhelt-extracted with toluene-ethanol mixture (2:1 v/v) for 48 hours and dried in an oven at 50 ^oC for overnight and regarded as virgin coconut pith (VCP). Moreover, chemical modification of VCP was executed by grafting γ-APS (0.1 M) solution. In the first step, a miscible mixture of ethanol and water (80:20) was stirred and then γ-APS (alkaline pH) was added to the above prepared mixture, which will lead to the hydrolysis of silane. After some period of time, VCP (0.5 g) was added to be modified by γ-APS. The mixture was stirred for 2 hours (500 rpm) followed by drying at 60 ^oC for overnight and regarded as grafted coconut pith (GCP).

Adsorption Experiments

Batch adsorption experiments were conducted by placing adsorbent (0.05 g) in 100 mL flask containing 50 mL (10 to 500 mg/L) of Au(III) at pH 4.00. The bottles were shaken at 200 rpm for 2 days using a mechanical shaker to achieve equilibrium. The mixture was filtered by nylon syringe filter 0.80 µm to remove adsorbent particles. After filtration, the concentration of Au(III) was determined by atomic absorption spectrophotometer (AAS) (Model Perkin-Elmer precisely HGA 900). The amount of Au(III) adsorbed at equilibrium q_e (mg/g) was calculated by equation 1:

$$q_e = \left(\frac{(C_o - C_e)V}{m}\right) \qquad (1)$$

where C_o and C_e (mg/L) are the initial and the equilibrium concentrations of Au (III). V is the volume of gold solution (L) and m is the mass of adsorbent used (g). Kinetic studies were done by mixing 0.05 g of VCP and GCP with 50 mL of Au(III) solution (50 mg/L, pH = 4.00) and taking samples at different time intervals (1-2880 min). The amount of Au(III) adsorbed at time t, q_t (mg/g) was calculated by equation 2:

$$q_t = \left(\frac{(C_o - C_t)V}{m}\right) \qquad (2)$$

Where C_o and C_t are the initial and final concentration of Au (III) at time t, respectively. Three batch adsorption cycles were conducted to study durability and regenerability of the adsorbents. This was performed by mixing adsorbents (0.250 g) with 250 mL (250 mg/L) of Au(III) solution. The spent adsorbents (VCP and GCP) were filtered and rinsed with deionized water to remove traces of gold and dried in an oven at 50 ^oC for overnight. After that, washing was performed with eluting agent, NaOH (1.0M). The mixture was shaken at 200 rpm for 2 days, followed by filtering to separate adsorbent from the alkali solution. The adsorbent was dried in an oven at 50 ^oC and executed again an adsorption cycle. The experimental scheme for the preparation of adsorbent and the adsorption experiments for the uptake of Au(III) ions is shown in Fig. 1.

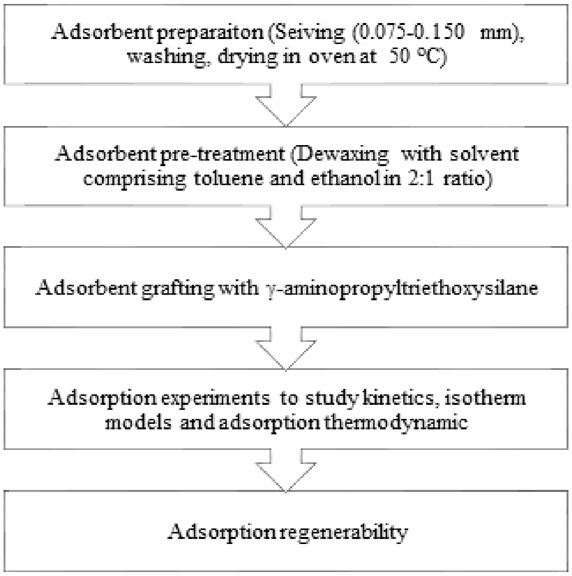

Fig. 1: Experimental scheme for the adsorption of Au(III) ions by grafted coconut pith.

Results and Discussion

Adsorption Isotherm

The study on adsorption isotherm describes the relation between the adsorbate concentration in the bulk and the adsorbed amount on the interface [33]. The isotherm study is conducted by fitting experimental data to different isotherm models (Langmuir, Freundlich, Temkin and Dubinin-Radushkevich) and selecting the suitable model for design purposes [34]. The Langmuir adsorption model considers the various phenomenon such as: adsorption is occurring on a monolayer alone, all binding sites are similar and can adsorb only one atom per active site, and the rate of adsorption of one molecule to a binding site have no effect from its adjacent site occupancy [34-36]. The mathematical expression of Langmuir model is described by equation 3:

$$q_e = q_{max} \frac{K_L C_e}{1+K_L C_e} \quad (3)$$

where q_e (mg/g) and C_e (mg/L) is the equilibrium metal concentration on the adsorbent and in the solution, respectively. While, q_{max} is the maximum amount of the metal adsorbed per gram of adsorbent (mg/g) and K_L (constant) is solely related to the affinity of the binding sites (L/mg). Langmuir equation in the linearized form is described by equation 4:

$$\frac{C_e}{q_e} = \frac{C_e}{q_{\max}} + \frac{1}{q_{\max} K_L} \quad (4)$$

The linear plot between specific adsorption (C_e/q_e) against C_e showed higher correlation factor ($R^2 > 0.98$) and Langmuir constants (q_{max} and K_L) were determined from the slope and intercept of the plot (Table-2). The separation factor (R_L) determines the favorability of the adsorption isotherm and described by equation 5:

$$R_L = \frac{1}{1+K_L C_0} \quad (5)$$

where C_o is the highest initial metal concentration of adsorbate (mg/L) and K_L (L/mg) is Langmuir constant. R_L indicates the shape of isotherm to be either unfavorable ($R_L > 1$), favorable ($0 < R_L < 1$), linear ($R_L = 1$) or irreversible ($R_L = 0$). The value of R_L for both VCP and GCP adsorbents is between 0 and 1, which indicates the favorability of the Au(III) adsorption on VCP and GCP adsorbents (Table-2). The adsorption behavior of organic and inorganic compounds for different types of adsorbent is explained using Freundlich isotherm [35]. In this model, heterogeneity of the surface and multilayer adsorption on the binding sites located on the adsorbent surface is discussed [34,37,38]. The mathematical expression for the Freundlich isotherm is described by equation 6:

$$\log q_e = \log K_F + \frac{1}{n} \log C_e \quad (6)$$

where K_F ((mg/g) (L/mg)$^{1/n}$) is the adsorption capacity of the adsorbent and n indicates the favorability of the adsorption process. Moreover, values of K_F and n are calculated from the slop and intercept of the plot ($\log q_e$ versus $\log C_e$). On average, the values of n between 1 and 10 expresses the favorability of adsorption process, while larger value of n (smaller values of 1/n) indicates the presence of strong interaction between adsorbate and adsorbent.

Temkin and Pyzhev isotherm model discusses the influence of interactions between adsorbent and adsorbate that are responsible for the linear decrease in adsorption heats with surface coverage [38, 39]. Temkin isotherm mathematical form is described by equation 7:

$$q_e = \left(\frac{RT}{b}\right) \ln A C_e \quad (7)$$

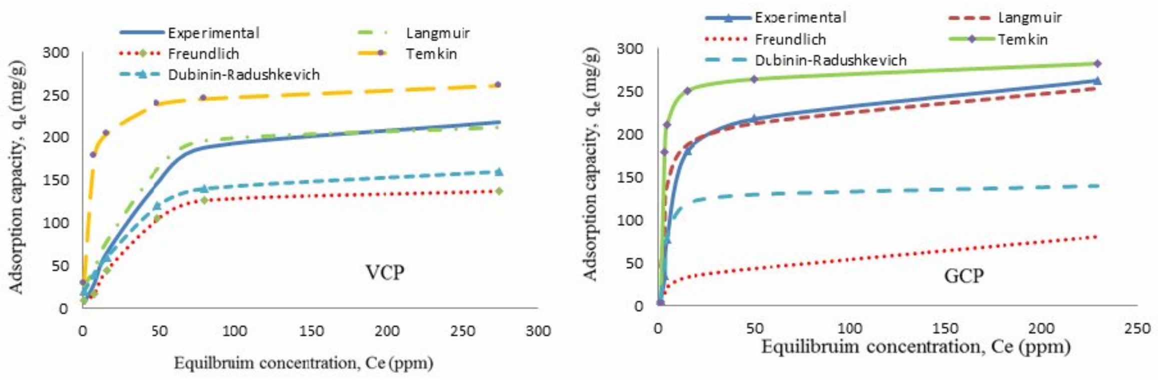

Fig. 2: Isotherm models analysis of Au(III) adsorption onto VCP and GCP adsorbents (m = 0.05g, pH = 4.00, temp. 30 °C).

Table-2: Isotherm model parameters for Au(III) adsorption onto VCP and GCP adsorbents.

Isotherm models	Parameters	Values	
		VCP	GCP
Experimental	q_e^{a}	217.4	262.5
Langmuir	q_{max}^{a}	256.41	285.59
	K_L^{b}	0.0218	0.0480
	R_L^{c}	0.47	0.019
	R^2	0.9889	0.9811
Freundlich	K_F^{d}	2.37	3.354
	$1/n^{c}$	0.8645	0.628
	R^2	0.9439	0.7812
Temkin	A^{e}	1.95	1.09
	B^{c}	43.71	51.33
	R^2	0.9163	0.9494
Dubinin-Radushkevich	q_{max}^{a}	1557.44	2213.9
	β f	5.00	6.00
	R^2	0.9738	0.8429

a: mg/g; b: L/mg; c: dimensionless; d: ((mg/g) $(L/mg)^{1/n}$); e: L/g; f: (mol^2/kJ^2) x 10^9

The linearized form of equaiton is shown in equation 8:

$$q_e = B\ln A + B \ln C_e \tag{8}$$

where b (Temkin constant) describes the heat of adsorption (J/mol), while B= RT/b. Both Temkin constants A(L/g) and B(dimensionless) can be determined from the intercept and slope of linear plot of q_e versus $\ln C_e$, respectively and their values are mentioned in Table-2. Dubinin and co-workers proposed a model for the subcritical vapors in micropore solids, where adsorption follows pore filling mechanism onto energetically non-uniform surface. The Dubinin–Radushkevich (DR) equation describes the relation between the adsorption curve and porous structure of the adsorbent [35,40-42]. The mathematical expression for the DR-isotherm is described in equation 9:

$$\ln q_e = \ln q_{max} - \beta\varepsilon^2 \tag{9}$$

where β (mol^2/KJ^2) is DR constant and ε is polyani potential described as $\varepsilon = RT\ln(1+1/C_e)$. The values of DR constant (β) (slope) and q_{max} (intercept) were calculated from the plot among ε^2 and $\ln q_e$ (Table-2). Maximum adsorption capacity q_{max} (mg/g) calculated from this isotherm does not fit well with the experimental q_e (mg/g). The comparison of Langmuir, Freundlich, Temkin and DR isotherms with the experimental data of Au(III) adsorption on VCP and GCP adsorbents is displayed in Fig. 2.

The study of the various isotherm models (Table-2 and Fig. 1) leads to the conclusion that Langmuir isotherm well fitted the experimental data due to its high correlation coefficient ($R^2 > 0.99$), whereas, the low correlation coefficients ($R^2 < 0.96$) for Freundlich, Temkin and DR isotherm showed poor agreement with experimental data. The mono layer adsorption capacity according to Langmuir isotherm model was 256.41 and 285.59 (mg/g) for VCP and GCP, respectively. The suitability of the Langmuir isotherm model for Au(III) adsorption can be attributed to the uniform adsorbent surface having equivalent adsorption affinity for adsorbate. The previously studied adsorbents for Au(III) adsorption are listed in Table-3 along with their suggested isotherm and kinetic models [1,13,14,23-31,43-49].

Adsorption Kinetics

In this section, mechanism of Au(III) adsorption on coconut pith adsorbents and rate-controlling steps were determined by adsorption kinetics [34]. The study showed that a large quantity (80%) of Au(III) ions were removed in the earlier duration of adsorption (30 min). However, the slow rate of attainment of equilibrium indicates the presence of large number of binding site initially available for the adsorption; but thereafter, there will be a competition between metal ions on the adsorbent surface and bulk phase for vacant sites [39]. The Lagergren pseudo-first order model describes that the rate of adsorption is proportional to the number of sites occupied by the adsorbate and described in equation 10 [50]:

$$\ln(q_e - q_t) = \ln q_e - k_1 t \qquad (10)$$

where q_e and q_t are the amounts of Au(III) adsorbed (mg/g) at equilibrium and time t (min), respectively and k_1 (min^{-1}) is the pseudo-first order rate constant. The adsorption rate constant (k_1) for Au(III) adsorption was calculated experimentally by plotting $\ln(q_e-q_t)$ versus t for VCP and GCP adsorbents (Table-4). The theoretical values are far smaller than experimental data (Table-4), suggesting that pseudo-first order model does not fit well to experimental data. This lack of fit suggests the presence of external resistance controlling the pace at the start of adsorption process [35].

Ho and Mckay [51] noticed that pseudo-first order model was not suitable to explain the entire adsorption period. Thus, they proposed pseudo-second order model based on the assumption that adsorption follows the second-order chemisorption path. The mathematical form of the pseudo-second order model is described in equation 11:

$$\frac{t}{q_t} = \frac{1}{k_2 q_e^2} + \frac{1}{qe} t \qquad (11)$$

where k_2 is the pseudo-second order equilibrium rate constant. The slope and intercept of the linear plot t/q_t versus t yield the values of q_e and k_2. The calculated q_e values matched well with the experimental data and correlation coefficients (R^2) values were close to 1 (Table-4). Hence, the adsorption of Au(III) ions could be fitted more favorably by pseudo-second order kinetic model.

Elovich equation was applied to kinetic data of Au(III) adsorption, which describes the chemical adsorption mechanism in nature and assumes solid surface activation energy for chemisorption. The Elovich equation is described in equation 12 [52]:

$$q_t = (1/\beta) \ln\alpha\beta + (1/\beta) \ln t \qquad (12)$$

where α (mg/g min) and β (g/mg) are related to initial adsorption rate and desorption constant. The parameters (α and β) were determined (Table-4) by the linear plot (q_t versus lnt) for VCP and GCP adsorbents. The comparison of three kinetic models for Au(III) adsorption onto VCP and GCP adsorbents (Fig. 3), indicated that pseudo-second order model fitted the empirical data well and R^2 for pseudo-second order model is too high, compared to other kinetic models. This was also concluded that Au(III) adsorption was chemisorption according to the pseudo-second order model assumption. Chemisorption is a type of adsorption that is driven by chemical reaction generating new compounds on the adsorbent surface opposite to the physical adsorption in which the chemical species of the adsorbate and surface remain unchanged [35].

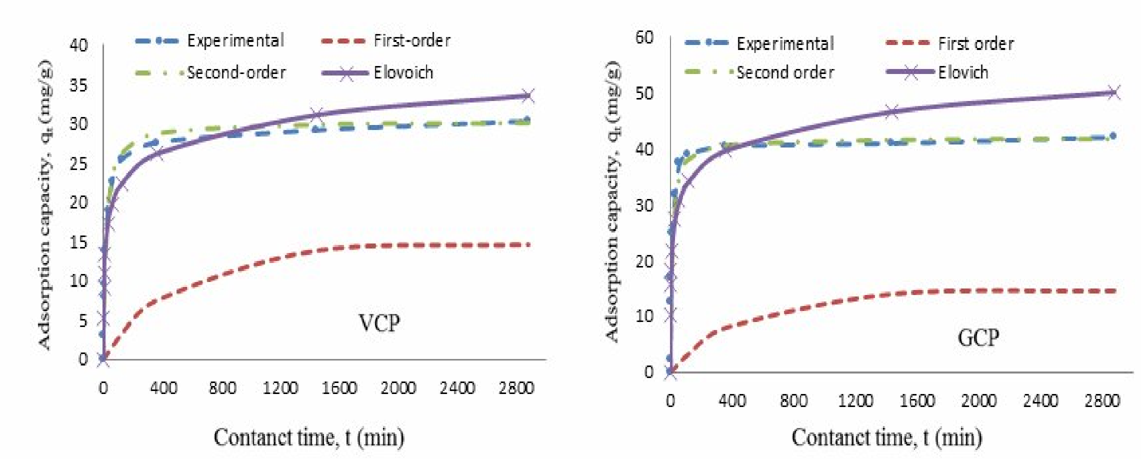

Fig. 3: Kinetic models analysis of Au(III) adsorption onto VCP and GCP adsorbents (C_o = 50 mg/L, m = 0.05g, pH = 4.00, temp. 30 °C).

Table-3:Literature comparison of the gold adsorption capacity, isotherm and kinetic models.

Adsorbent	q_m (mg/g)	Isotherm model	Kinetic model	Reference
Chemically modified chitosan resin	**709.05**	**Langmuir**	**PS2**	**[23]**
EN-lignin	**606.63**	**Langmuir**	**-**	**[43]**
PA-lignin	**384.07**			
Ovalbumin	**36±5**	**-**	**-**	**[44]**
BSA	**40±2**			
Lysozyme	**19±2**			
Lignophenol gel	**378.16**	**Langmuir**	**-**	**[24]**
Immobilized fungal biomass	**94.34**	**Langmuir and Freundlich**	**-**	**[31]**
Silk sericin	**196.96**	**-**	**-**	**[45]**
chitosan	**649.96**			
L-lysine modified cross-linked chitosan resin	**70.34**	**Langmuir**	**PS2**	**[46]**
Durio zibethinus husk	**339.55**	**Langmuir**	**PS2**	**[1]**
Cross-linked gel	**1516.59**	**BET**	**PS1**	**[14]**
Crude tannin powder	**1142.36**			
Cladosporium cladosporioides biomass bead	**100**	**Freundlich**	**-**	**[47]**
Bacterial (Bacillus stubilis)	**1.57**	**-**	**-**	**[48]**
Fungal (penicillium chrysogenum)	**1.41**			
Seawood biomass (sargassum fluitans)	**0.630**			
Rice husk carbon	**149.68**	**Langmuir**	**-**	**[25]**
Bisthiourea derivatives of resin	**714.96**	**Langmuir**	**-**	**[49]**
Alfalfa	**35.45**	**-**	**-**	**[26]**
Sulfur derivatives of chitosan	**630.27**	**Langmuir**	**PS1**	**[28]**
Egg shell membrane	**618.0**	**Langmuir**	**-**	**[27]**
Dealginated seaweed waste	**78.78**	**-**	**-**	**[30]**
Condensed tannin gel	**8000.0**	**-**	**PS1**	**[13]**
Calcium alginate beads	**290.0**	**-**	**-**	**[29]**
Coconut pith				
VCP	**256.41**	**Langmuir**	**PS2**	**This study**
GCP	**285.59**			

- : data not available in the paper; PS1: Pseudo-first order; PS2: Pseudo-second order.

Table-4: Adsorption kinetic models for Au(III) adsorption onto VCP and GCP adsorbents.

Kinetic models	Parameters	Values	
		VCP	**GCP**
Experimental	$q_e^{a}{}_{,exp}$	**31.5**	**41.94**
Pseudo-first order	$q_e^{a}{}_{,cal}$	**14.72**	**14.54**
	k_1^{b}	**0.0020**	**0.0022**
	R^2	**0.6869**	**0.51**
Pseudo-second order	$q_e^{a}{}_{,cal}$	**30.21**	**41.84**
	k_2^{b}	**0.001734**	**0.002036**
	R^2	**0.9997**	**0.9999**
Elovich	β^{c}	**0.28**	**0.20**
	α^{d}	**15.21**	**39.00**
	R^2	**0.9463**	**0.8512**
Weber-Morris	k_1^{b}	**4.92**	**10.19**
	R^2	**0.9827**	**0.9817**
	k_2^{b}	**1.14**	**1.29**
	R^2	**0.9665**	**0.8397**
	k_3^{b}	**0.078**	**0.0461**
	R^2	**0.9987**	**0.9415**
Film diffusion	D_1^{e}	**$7.33*10^{-8}$**	**$1.63*10^{-7}$**
	R^2	**0.9827**	**0.9817**
Pore diffusion	D_2^{e}	**$3.80*10^{-5}$**	**$5.65*10^{-5}$**
	R^2	**0.9236**	**0.9142**

a: mg/g; b: min^{-1}; c: g/mg; d: $mg/g.min^{0.5}$; e: cm^2/min.

Adsorption Mechanism

The kinetic data was fitted with Weber's intraparticle diffusion model to elucidate the adsorption mechanism for Au(III), which will be either boundary film (external film diffusion) or pores in the adsorbents. The mathematical form of Weber and Morris [53] model is described in equation 13:

$$q_t = k_{id}\, t^{0.5} + C \qquad (13)$$

where intercept C (mg/g) gives an estimate about the thickness of the boundary layer and k_{id} is the intraparticle diffusion constant, evaluated from the slop of a linear plot of q_t versus $t^{0.5}$. The straight line passing through the origin indicates that Au(III) adsorption will follow intraparticle diffusion mechanism [54], while the presence of multi-linear plots indicate that two or more steps are controlling the adsorption process. In this study, the data showed multi-linearity (Fig. 4) and the lines did not pass through origin, which indicates intraparticle diffusion was not solely a rate controlling step, either it was combination of external surface sorption and intraparticle diffusion [34,55]. The same multi-linearity was reported by Ofomaja et al. [56] and Waranusantigul et al. [57] for the adsorption of methylene blue onto various adsorbents.

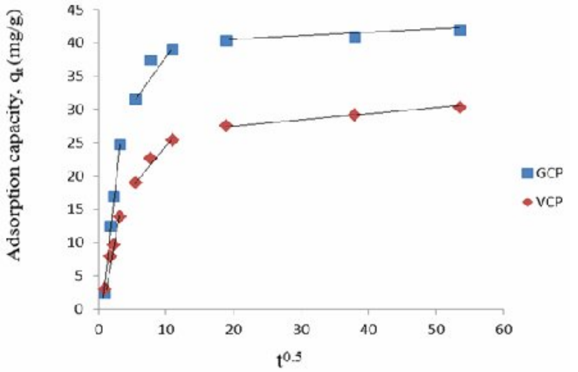

Fig. 4: Weber-Morris kinetic plot for Au(III) adsorption onto VCP and GCP adsorbent (C_o= 50 mg/L, m = 0.05g, pH = 4.00, temp. 30 °C).

The first sharper stage (0-10 min) describes the diffusion of adsorbate through the solution to the external surface of the adsorbent or the boundary layer diffusion of the adsorbate molecules. The second phase (10-120 min) describes that intraparticle diffusion is rate-limiting and the third stage (120-2880 min) also can be regarded as final equilibrium stage in which the intraparticle diffusion starts to slow down due to extremely low adsorbate concentration [55]. The three stages discussed above indicate that the adsorption process occurs by surface adsorption and intraparticle diffusion (meso- and micropores).

The intraparticle diffusion is assumed to be controlled by two phenomenons: film diffusion and pore diffusion. Different models were applied to determine film diffusion (D1) and pore diffusion (D2) coefficients. The linear equation for film diffusion is shown in equation 14.

$$\frac{q_t}{q_e} = 6\left(\frac{D_1}{\pi r^2}\right)^{0.5} t^{0.5} \qquad (14)$$

The film diffusion coefficient (D_1) was calculated from the slop of plot between q_t/q_e and $t^{0.5}$ (Table-4). However, pore diffusion coefficient (D_2) was calculated by the application of Boyd plot (Bt vs. time (t)). F is the ratio of adsorption capacity at time t and equilibrium (q_t/q_e). If the value of F > 0.8 then the below equation 15 is applied.

$$Bt = -\,0.04977 - \ln(1 - F) \qquad (15)$$

And if the value of F < 0.8 then the below equation 16 is applied

$$\mathbf{B_t = \sqrt{\pi} - \sqrt{\left[\pi - \left(\frac{\pi^2 F}{3}\right)\right]^2}} \qquad (16)$$

The slop (B) of the plot (Bt vs. t) indicates pore diffusion coefficient (D_2) from the equation 17.

$$\mathbf{B = \frac{D_2^2 \pi^2}{r^2}} \qquad (17)$$

The values of D_2 and R^2 for VCP and GCP adsorbents are listed in Table-4. The comparison of film diffusion (D_1) and pore diffusion (D_2) coefficients indicates that pore diffusion is faster than the film diffusion coefficients and similar results were reported by Johari et al., [58] and Onal et al., [59]. Furthermore, chemical structure of γ-APS and the modification effect of this aminofunctional silane coupling agent on the surface of coconut pith and adsorption of Au(III) ions is shown in Fig. 5.

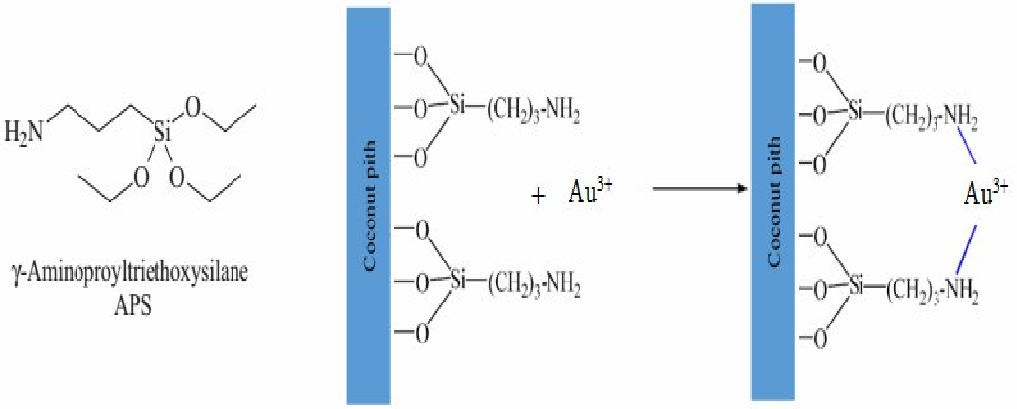

Fig. 5: Chemical structure of γ-APS and uptake of Au(III) ions by amine functional group.

Adsorption thermodynamics

The study of the influence of temperature on adsorption of Au(III) indicated an increase of adsorption capacity with the rise of temperature, which indicates endothermic nature of Au (III) adsorption on VCP and GCP adsorbents (Fig. 6). Temperature played a key role to enhance surface activity of the active binding sites and kinetic energy of solute [60].

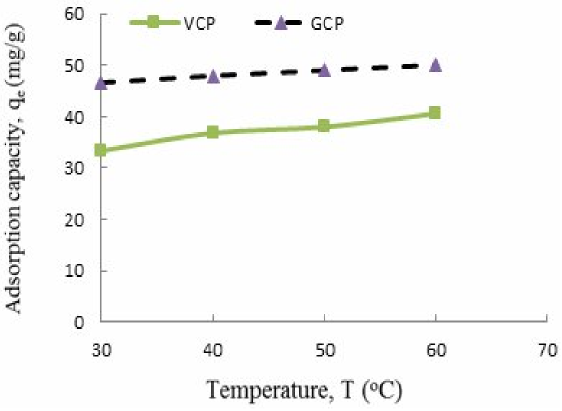

Fig. 6: Effect of temperature on Au(III) adsorption onto VCP and GCP adsorbents (C_o= 50 mg/L, m = 0.05g, pH = 4.00).

The set of thermodynamic parameters, such as, Gibbs free energy (ΔG^o), enthalpy (ΔH^o) and entropy (ΔS^o) were determined by the following Equations at different temperatures [34,55]:

$$\Delta G^o = \Delta H^o - T\Delta S^o \quad (18)$$

$$\ln \frac{q_e}{C_e} = \frac{-\Delta H^o}{RT} + \frac{\Delta S^o}{R} \quad (19)$$

where thermodynamic parameters (ΔH^o and ΔS^o) were determined from the slope and the intercept of the linear plot ($\ln q_e/C_e$ versus 1/T) (Fig. 7) and then values of ΔG^o were calculated. Therefore, negative values of ΔG^o describes the spontaneity of Au(III) adsorption process. However, positive values of ΔH^o and ΔS^o suggested the endothermic nature of the reaction and increased randomness at the solid/solution interface for Au(III) adsorption (Table-5) [34,61]. The higher entropy values for GCP adsorbent compared to VCP depicted the higher randomness of modified adsorbent.

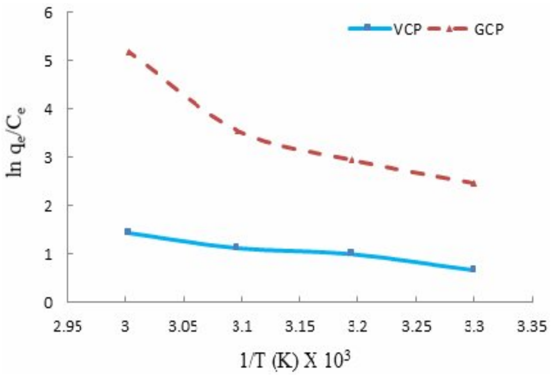

Fig. 7: Plot of $\ln q_e/C_e$ versus 1/T for estimation of thermodynamic parameters for the the adsorption of Au(III) on VCP and GCP adsorbents (C_o= 50 mg/L, m = 0.05g, pH = 4.00).

Table-5: Thermodynamic data for VCP and GCP adsorbents.

	ΔH◦ (kJ/mole)	**ΔS◦ (kJ/mole.K)**	**-ΔG◦ (kJ/mole)**			
			303 K	**313 K**	**323 K**	**333 K**
VCP	**0.02059**	**0.07361**	**22.28**	**23.01**	**23.75**	**24.49**
GCP	**0.07252**	**0.25814**	**78.10**	**80.68**	**83.26**	**85.84**

Adsorbent Regenerability

The reusability of the adsorbents is an important feature to make the adsorption process attractive and economical. In the present study, adsorption-desorption batch operations were conducted to exam the reusability of adsorbents for Au (III) ions. The results indicated that both adsorbents could be repeatedly recycled for 3-4 cycles with only a slight decrease in their initial adsorption capacities (Fig. 8). Moreover, modified adsorbent (GCP) exhibited a higher performance in its reusability compared to VCP adsorbent.

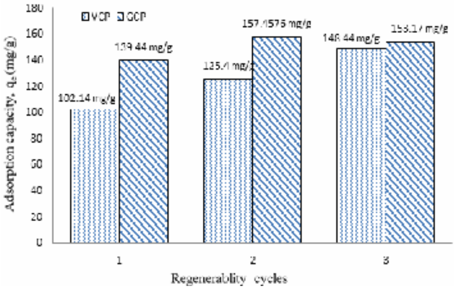

Fig. 8: Regenerability data of Au(III) for VCP and GCP adsorbents (C_o=250 mg/L, m = 0.250 g, pH = 4.00, temp. 30 °C).

Conclusion

In this work, coconut pith adsorbents exhibited an excellent affinity for Au(III) ions, especially modified coconut pith (GCP), which showed higher uptake capacity and reusability. The characterization of the adsorbents before and after adsorption cycles explained the morphology and structure of adsorbents in detail. The experimental data was well fitted by Langmuir isotherm, giving exhibiting a maximum adsorption capacity of 285.59 mg/g for GCP at 30 ^{o}C. Adsorption kinetics was well described by the pseudo-second order model. A thermodynamic study revealed the endothermic nature of Au (III) adsorption on VCP and GCP, which fitted well with the temperature study. Regenerability study for VCP and GCP showed a little loss in uptake capacity even after three cycles.

References

1. M. A. Z. Abidin, A. A. Jalil, S. Triwahyono, S. H. Adam and N. H. Nazirah Kamarudin, Recovery of Gold(III) from an Aqueous Solution onto a Durio Zibethinus Husk, *Biochem. Eng. J.* **54**, 124 (2011).
2. V. Sheoran, A. Sheoran and P. Poonia, Phytomining: A Review, *Miner. Eng.* **22**, 1007 (2009).
3. B. Moore, J. Duncan and J. Burgess, Fungal Bioaccumulation of Copper, Nickel, Gold and Platinum, *Miner. Eng.* **21**, 55 (2008).
4. K. Zaw, S. G. Peters, P. Cromie, C. Burrett and Z. Hou, Nature, Diversity of Deposit Types and Metallogenic Relations of South China, *Ore Geol. Rev.* **31**, 3 (2007).
5. L. Barbieri, R. Giovanardi, I. Lancellotti and M. Michelazzi, A New Environmentally Friendly Process for the Recovery of Gold from Electronic Waste, *Environ. Chem. Lett.* **8**, 171 (2010).
6. P. Chancerel, C. E. Meskers, C. Hagelüken and V. S. Rotter, Assessment of Precious Metal Flows during Preprocessing of Waste Electrical and Electronic Equipment, *J. Ind. Ecol.,* **13**, 791 (2009).
7. J. Cui and L. Zhang, Metallurgical Recovery of Metals from Electronic Waste: A Review, *J. Hazard. Mater.* **158**, 228 (2008).
8. B. S. Kim, J. C. Lee, J. Jeong, S. Kang and K. H. Lee, A High Temperature Process for Extracting Valuable Metals from Waste Electric and Electronic Scraps (WEES), *Mat. Tran.* **50**, 1558 (2009).
9. Y. J. Park and D. J. Fray, Recovery of High Purity Precious Metals from Printed Circuit Boards, *J. Hazard. Mater.* **164**, 1152 (2009).
10. V. H. Ha, J.-C. Lee, J. Jeong, H. T. Hai and M. K. Jha, Thiosulfate Leaching of Gold from Waste Mobile Phones, *J. Hazard. Mater.* **178**, 1115 (2010).
11. E. Most, Calling All Cell Phones, *Collection, Reuse, and Recycling Programs in the US, Inform Inc., New York* (2003).
12. T. Shirahase and A. Kida, Metals Contents in one Waste Personal Computer by Detailed Dismantling, *J. Jpn. Soc. Mat. Cy. Waste Manage.* **20**, 217 (2009).
13. T. Ogata and Y. Nakano, Mechanisms of Gold Recovery from Aqueous Solutions using a Novel Tannin Gel Adsorbent Synthesized from Natural Condensed Tannin, *Water Res.* **39**, 4281 (2005).
14. M. Gurung, B. B. Adhikari, H. Kawakita, K. Ohto, K. Inoue and S. Alam, Recovery of Au(III) by Using Low Cost Adsorbent Prepared from Persimmon Tannin Extract, *Chem. Eng. J.* **174**, 556 (2011).
15. J. L. Cortina, A. Warshawsky, N. Kahana, V. Kampel, C. H. Sampaio and R. M. Kautzmann, Kinetics of Goldcyanide Extraction Using Ion-Exchange Resins containing Piperazine Functionality, *React. Funct. Polym.* **54**, 25 (2003).
16. M. Sánchez-Loredo and M. Grote, Carboxyl-Substituted Derivatives of 5-Decyl Dithizone as Solvent Extractants for Precious Metal Ions, *Solvent Extr. Ion Exch.* **18**, 55 (2000).
17. P. Sorensen, Gold Recovery from Carbon-in-Pulp Eluates by Precipitation with a Mineral Acid III. The Acid Precipitation Step in Applications, *Hydrometallurgy* **21**, 249 (1988).
18. B. Volesky, Detoxification of Metal-Bearing Effluents: Biosorption for the Next Century, *Hydrometallurgy* **59**, 203 (2001).
19. C. Mack, B. Wilhelmi, J. Duncan and J. Burgess, Biosorption of Precious Metals, *Biotechnol. Adv.* **25**, 264 (2007).
20. W. Wan Ngah and M. Hanafiah, Adsorption of Copper on Rubber (Hevea Brasiliensis) Leaf Powder: Kinetic, Equilibrium and Thermodynamic Studies, *Biochem. Eng. J.* **39**, 521 (2008).
21. J. Lehrfeld, Conversion of Agricultural Residues into Cation Exchange Materials, *J. Appl. Polym. Sci.* **61**, 2099 (1996).
22. J. S. Levine. Biomass Burning and Global Change: Remote Sensing, Modeling and Inventory Development, and Biomass Burning In Africa, Vol. 1. MIT Press, (1996).

23. A. M. Donia, A. A. Atia and K. Z. Elwakeel, Recovery of Gold (III) and Silver (I) on a Chemically Modified Chitosan with Magnetic Properties, *Hydrometallurgy* **87**, 197 (2007).
24. D. Parajuli, K. Inoue, H. Kawakita, K. Ohto, H. Harada and M. Funaoka, Recovery of Precious Metals using Lignophenol Compounds, *Miner. Eng.* **21**, 61 (2008).
25. R. Chand, T. Watari, K. Inoue, H. Kawakita, H. N. Luitel, D. Parajuli, T. Torikai and M. Yada, Selective Adsorption of Precious Metals from Hydrochloric Acid Solutions using Porous Carbon Prepared from Barley Straw and Rice Husk, *Miner. Eng.* **22**, 1277 (2009).
26. G. Gamez, J. L. Gardea Torresdey, K. J. Tiemann, J. Parsons, K. Dokken and M. Jose Yacaman, Recovery of Gold(III) from Multi-Elemental Solutions by Alfalfa Biomass, *Adv. Environ. Res.* **7**, 563 (2003).
27. S. I. Ishikawa, K. Suyama, K. Arihara and M. Itoh, Uptake and Recovery of Gold Ions from Electroplating Wastes using Eggshell Membrane, *Bioresour. Technol.* **81**, 201 (2002).
28. M. L. Arrascue, H. M. Garcia, O. Horna and E. Guibal, Gold Sorption on Chitosan Derivatives, *Hydrometallurgy* **71**, 191 (2003).
29. E. Torres, Y. Mata, M. Blazquez, J. Munoz, F. Gonzalez and A. Ballester, Gold and Silver Uptake and Nanoprecipitation on Calcium Alginate Beads, *Langmuir* **21**, 7951 (2005).
30. M. E. Romero-González, C. J. Williams, P. H. Gardiner, S. J. Gurman and S. Habesh, Spectroscopic Studies of the Biosorption of Gold (III) by Dealginated Seaweed Waste, *Environ. Sci. Technol.* **37**, 4163 (2003).
31. K. M. Khoo and Y. P. Ting, Biosorption of Gold by Immobilized Fungal Biomass, *Biochem. Eng. J.* **8**, 51 (2001).
32. M. Abdelmouleh, S. Boufi, A. ben Salah, M. N. Belgacem and A. Gandini, Interaction of Silane Coupling Agents with Cellulose, *Langmuir* **18**, 3203 (2002).
33. J. Eastoe and J. S. Dalton, Dynamic Surface Tension and Adsorption Mechanisms of Surfactants at the Air–Water Interface, *Adv. Colloid Interface Sci.* **85**, 103 (2000).
34. Z. Y. Yao, J. H. Qi and L. H. Wang, Equilibrium, Kinetic and Thermodynamic Studies on the Biosorption of Cu (II) onto Chestnut Shell, *J. Hazard. Mater.* **174**, 137 (2010).
35. J. Febrianto, A. N. Kosasih, J. Sunarso, Y. H. Ju, N. Indraswati and S. Ismadji, Equilibrium and Kinetic Studies in Adsorption of Heavy Metals using Biosorbent: A Summary of Recent Studies, *J. Hazard. Mater.* **162**, 616 (2009).
36. V. S. Munagapati, V. Yarramuthi, S. K. Nadavala, S. R. Alla and K. Abburi, Biosorption of Cu(II), Cd(II) and Pb(II) by Acacia Leucocephala Bark Powder: Kinetics, Equilibrium And Thermodynamics, *Chem. Eng. J.* **157**, 357 (2010).
37. A. Witek-Krowiak, R. G. Szafran and S. Modelski, Biosorption of Heavy Metals from Aqueous Solutions onto Peanut Shell as a Low-Cost Biosorbent, *Desalination* **265**, 126 (2011).
38. B. H. Hameed, D. K. Mahmoud and A. L. Ahmad, Equilibrium Modeling and Kinetic Studies on the Adsorption of Basic Dye by a Low-Cost Adsorbent: Coconut (Cocos Nucifera) Bunch Waste, *J. Hazard. Mater.* **158**, 65 (2008).
39. V. K. Gupta, A. Rastogi and A. Nayak, Biosorption of Nickel onto Treated Alga (Oedogonium hatei): Application of Isotherm and Kinetic Models, *J. Colloid Interface Sci.* **342**, 533 (2010).
40. A. Dada, A. Olalekan, A. Olatunya and O. DADA, Langmuir, Freundlich, Temkin and Dubinin–Radushkevich Isotherms Studies of Equilibrium Sorption of Zn^{2+} unto Phosphoric Acid Modified Rice Husk, *IOSR J.Appl. chem.* **3**, 38 (2012).
41. K. Y. Foo and B. H. Hameed, Insights into the Modeling of Adsorption Isotherm Systems, *Chem. Eng. J.* **156**, 2 (2010).
42. K. Vijayaraghavan, T. V. N. Padmesh, K. Palanivelu and M. Velan, Biosorption of Nickel(II) Ions onto Sargassum Wightii: Application of two-Parameter and Three-Parameter Isotherm Models, *J. Hazard. Mater.* **133**, 304 (2006).
43. D. Parajuli, H. Kawakita, K. Inoue and M. Funaoka, Recovery of Gold (III), Palladium (II), and Platinum (IV) by Aminated Lignin Derivatives, *Ind.Eng.Chem.Res.* **45**, 6405 (2006).
44. T. Maruyama, H. Matsushita, Y. Shimada, I. Kamata, M. Hanaki, S. Sonokawa, N. Kamiya and M. Goto, Proteins and Protein-Rich Biomass as Environmentally Friendly Adsorbents Selective for Precious Metal Ions, *Environ. Sci. Technol.* **41**, 1359 (2007).
45. X. Chen, K. F. Lam, S. F. Mak and K. L. Yeung, Precious Metal Recovery by Selective Adsorption Using Biosorbents, *J. Hazard. Mater.* **186**, 902 (2011).
46. K. Fujiwara, A. Ramesh, T. Maki, H. Hasegawa and K. Ueda, Adsorption of Platinum (IV), Palladium (II) and Gold (III) from Aqueous Solutions onto L-Lysine Modified Crosslinked Chitosan Resin, *J. Hazard. Mater.* **146**, 39 (2007).

47. A. V. Pethkar and K. M. Paknikar, Recovery of Gold from Solutions using Cladosporium Cladosporioides Biomass Beads, *J. Biotechnol.* **63**, 121 (1998).
48. H. Niu and B. Volesky, Characteristics of Gold Biosorption from Cyanide Solution, *J.Chem.Technol. Biotechnol.* **74**, 778 (1999).
49. A. A. Atia, Adsorption of Silver(I) and Gold(III) on Resins Derived from Bisthiourea and Application to Retrieval of Silver Ions from Processed Photo Films, *Hydrometallurgy* **80**, 98 (2005).
50. S. Lagergren, About the Theory of So-called Adsorption of Soluble Substances, *Kungliga Svenska Vetenskapsakademiens. Handlingar* **24**, 1 (1898).
51. Y. Ho and G. McKay, The Kinetics of Sorption of Basic Dyes from aqueous Solution by Sphagnum Moss Peat, *Can. J. Chem. Eng.* **76**, 822 (1998).
52. Y. S. Ho and G. McKay, A Comparison of Chemisorption Kinetic Models Applied to Pollutant Removal on Various Sorbents, *Process Saf. Environ. Prot.* **76**, 332 (1998).
53. W. Weber and J. Morris, Kinetics of Adsorption on Carbon from Solution, *J. Sanit. Eng. Div. Am. Soc. Civ. Eng* **89**, 31 (1963).
54. V. Poots, G. McKay and J. Healy, The Removal of Acid Dye from Effluent using Natural Adsorbents-I peat, *Water Res.* **10**, 1061 (1976).
55. A. E. Ofomaja, Intraparticle Diffusion Process for Lead(II) Biosorption onto Mansonia Wood Sawdust, *Bioresour. Technol.* **101**, 5868 (2010).
56. A. E. Ofomaja, Kinetic Study and Sorption Mechanism of Methylene Blue and Methyl Violet onto Mansonia (Mansonia Altissima) Wood Sawdust, *Chem. Eng. J.* **143**, 85 (2008).
57. P. Waranusantigul, P. Pokethitiyook, M. Kruatrachue and E. Upatham, Kinetics of Basic Dye (Methylene Blue) Biosorption by Giant Duckweed (Spirodela Polyrrhiza), *Environ. Pollut.* **125**, 385 (2003).
58. K. Johari, N. Saman, S. T. Song, H. Mat and D. C. Stuckey, Utilization of Coconut Milk Processing Waste as a Low-Cost Mercury Sorbent, *Ind.Eng.Chem.Res.* **52**, 15648 (2013).
59. Y. Önal, C. Akmil-Başar and Ç. Sarıcı-Özdemir, Investigation Kinetics Mechanisms of Adsorption Malachite Green onto Activated Carbon, *J. Hazard. Mater.* **146**, 194 (2007).
60. K. Vijayaraghavan and Y. S. Yun, Bacterial Biosorbents and Biosorption, *Biotechnol. Adv.* **26**, 266 (2008).
61. C. Namasivayam and D. Kavitha, Removal of Congo Red from Water by Adsorption onto Activated Carbon Prepared from Coir Pith, an Agricultural Solid Waste, *Dyes Pigments.* **54**, 47 (2002).